

## D-24 BACKSCATTERING CHARACTERISTICS OF BRIDGES FROM HIGH-RESOLUTION X-BAND SAR IMAGERY

Wen LIU, Kanako SAWA, and Fumio YAMAZAKI

Department of Urban Environment System, Chiba University  
1-33 Yayoi-cho, Inage-ku, Chiba 263-8522, Japan; wen.liu@chiba-u.jp

**ABSTRACT:** As the advances in the sensor technology, high-resolution SAR imagery data have been available to distinguish man-made objects in urban areas. Bridges are important elements of the traffic network. In this study, the fundamental investigation was carried out to clarify backscattering characteristics of bridges over water in TerraSAR-X satellite images and Pi-SAR2 aerial images. Sixteen bridges around Tokyo, Japan, were selected as the targets. The relationship between those phenomena and the acquisition conditions was discussed by comparing several SAR images. By grasping the backscatter characteristics of the bridges, the possibility of detecting bridge damages from SAR images was indicated.

**KEY WORDS:** TerraSAR-X, Pi-SAR2, double-bounce, triple-bounce, backscatter modelling

### 1. INTRODUCTION

In the recent decades, remote sensing has been used to monitor urban environment and to estimate damaged areas after disasters. Synthetic aperture radar (SAR), which can operate all day under all weather conditions, is an effective tool for emergency response. Owing to the development of the sensor technology, high-resolution SAR images have been available to observe man-made objects in the urban environment. Various damage detection methods for buildings using multi-temporal SAR images taken before and after a disaster have been proposed (Dong and Shan, 2013; Brett and Guida, 2013). However, fewer studies focus on bridges, which are core elements of urban infrastructure. Soergel et al. (2006) attempted to detect bridges over water from the airborne Interferometric SAR (InSAR) data set. Sousa et al. (2014) and Lazecky et al. (2017) monitored the deformation of bridges using the persistent scatter interferometry technique. Those researches require more than two SAR scenes. For the emergency response after disasters, the pre-event SAR images are not always available. Thus, the observation of bridges from a single SAR image is an important issue.

In this study, the backscattering characteristics of various bridges over water were investigated by observing sixteen bridges around Tokyo, Japan, using TerraSAR-X (TSX) satellite and Pi-SAR2 aerial images. The relationship between the projection characteristics of bridges and the acquisition conditions of SAR data was also discussed.

### 2. BACKSCATTER MODEL OF BRIDGES

According to Soergel et al. (2006), usually three parallel lines can be observed for a bridge over water in the high-resolution SAR images. First, the direct backscatter from a bridge, which is the layover of the bridge over water. Second one is the double-bounce

reflection between the bridge and water, which is located behind the first one in the range direction. The third one is the triple reflection, where the signal reaches water, a lower part of the bridge and water again. The backscatter model is shown in Fig. 1(a). This kind of backscatter model could be observed for large bridges that are in the high elevation from the water. However, for small bridges without enough heights, the three backscatter signals are overlapped as the model shown in Fig. 1(b). Then the

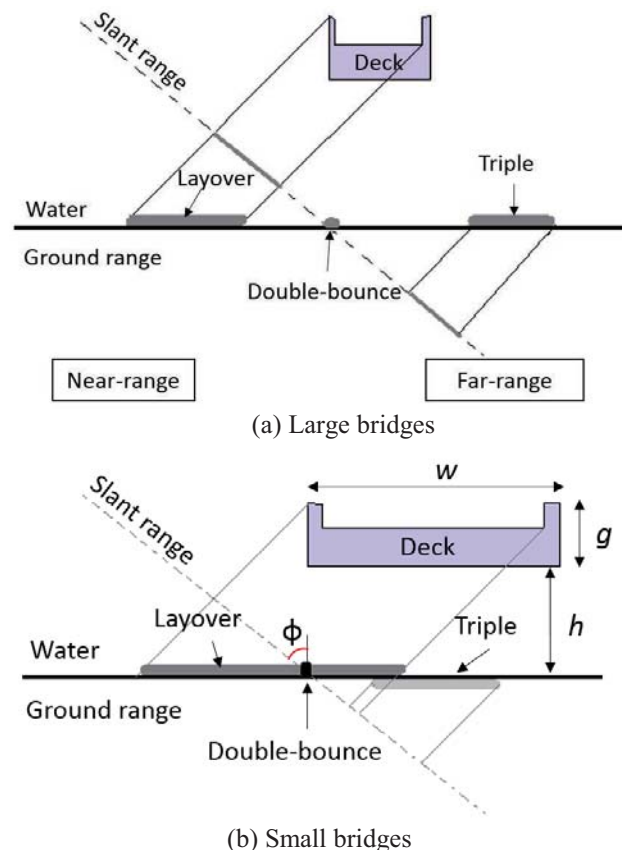


Figure 1. Backscatter models of bridges over water

bridges show up as salient bright lines surrounding the water surface in SAR images. This kind of backscatter model can be observed under the condition:

$$g + 2h < w \tan \phi \quad (1)$$

**Figure 1** shows the models when the range direction is orthogonal to the bridge. Usually, the azimuth direction of SAR does not match with the bridge's axial direction. Thus, the illumination angle ( $\theta$ ) between the range and bridge-axial direction, shown in **Fig. 2**, is another important element for appearance of bridges in SAR images.

In this study, four large bridges where three backscattering lines can be observed theoretically, and twelve small bridges where the backscatter signals overlapped, were used to discuss their performances in SAR data and the influence of the illumination angle. All the target bridges are located around Tokyo Bay.

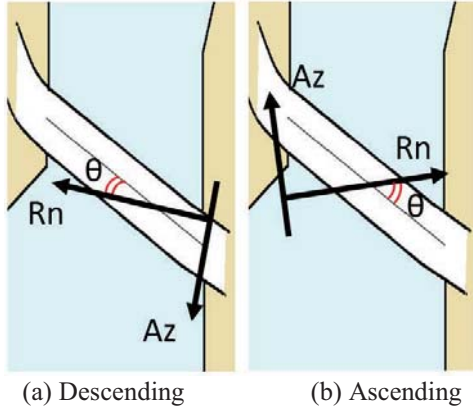


Figure 2. Illumination angle ( $\theta$ ) between the range and bridge-axial direction

### 3. BACKSCATTER CHARACTERISTICS OF LARGE BRIDGES

Rainbow bridge (I), Tokyo Gate bridge (II), Tsurumitsubasa bridge (III) and Yokohama Bay bridge (IV) were used as the examples of large bridges. The locations of the bridges are shown in **Fig. 3**. According to their structure scales, three parallel backscatter lines can be observed in the SAR image theoretically. The behaviour of these bridges was estimated using one TSX image and three Pi-SAR2 images. The acquisition conditions of the used SAR images are shown in **Table 1**.

Examples of Yokohama Bay (cable-styled) bridge in the TSX and Pi-SAR2 images are shown in **Fig. 4**. An aerial photo taken by the Geospatial Information Authority of Japan (GSI) is shown in **Fig. 4(a)**. The illumination angles for those three SAR images are  $71^\circ$  (b),  $79^\circ$ (c), and  $83^\circ$  (d), respectively. From the near-range to the far-range, the layover, double-bounce and triple-bounce reflection could be confirmed clearly in all the SAR images. Besides the backscatter from the deck, the layovers of the towers are also visible. Since the incident angle of Pi-SAR2 image taken on March 31, 2011 is larger than those for the TSX image and the Pi-SAR

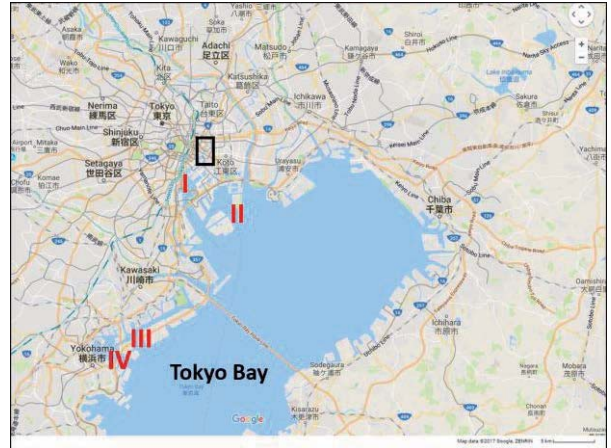


Figure 3. Locations of large bridges (I-IV) and small bridges (within the black square) on Google Map.

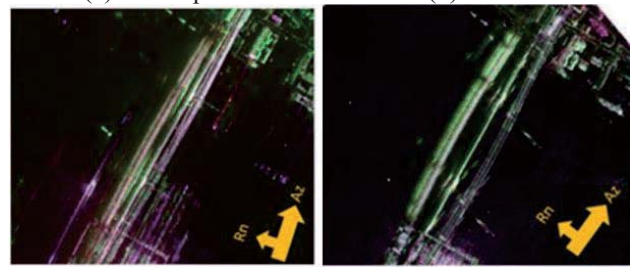
Table 1. Acquisition conditions of the SAR images

Sensor	Date	Incident angle [°]	Heading angle [°]	Resolution (R×A) [m]
TSX	2010/11/22	42.8	189.6	3.0×3.0
Pi-SAR2	2011/03/31	51.0	18.2	0.4×0.3
Pi-SAR2	2013/01/10	31.0	36.1	0.6×0.3
Pi-SAR2	2013/01/10	59.5	267.3	0.3×0.3
TSX	2008/02/15	42.19	189.61	1.8×1.5
TSX	2008/02/16	39.43	350.15	1.0×1.2



(a) Aerial photo

(b) TSX



(c) Pi-SAR2 (2011/03/31)

(d) PiSAR-2 (2013/01/10)

Figure 4. Yokohama Bay bridge

Table 2. Backscatter behaviour of the four large bridges

$\theta$ [°]	Bridge	Sensor	Number of lines	Double-bounce	Triple
11	I	TSX	1	×	×
38	III	TSX	1	×	△
46	III	Pi-SAR2	2	×	○
51-66	II	TSX	2	△	△
64	III	Pi-SAR2	5	○	○
67	I	Pi-SAR2	3	○	○
71	IV	TSX	3	○	○
77-88	II	Pi-SAR2	3	○	△
79	IV	Pi-SAR2	3	○	○
83	IV	Pi-SAR2	4	○	○

image on January 10, 2013, the distance between the three backscatter lines are closer than the others. In Fig. 4(d), a weak backscatter line could be observed in the far-range behind the triple reflection. We counted it as the fourth backscatter line, which is considered as the ambiguity (Liu and Yamazaki, 2011).

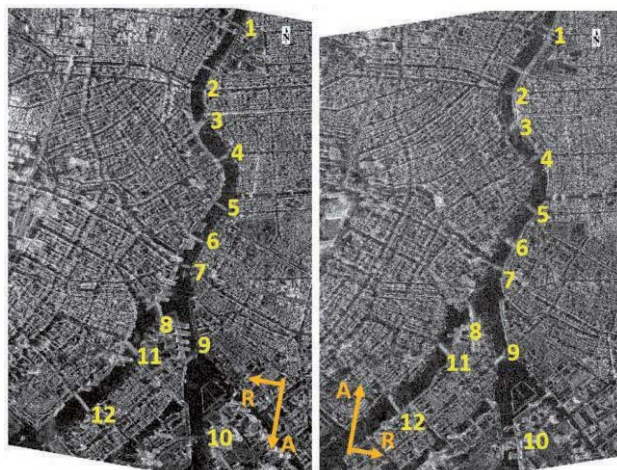
The number of the backscatter lines and the appearance of double-bounce and triple-bounce reflections under the different observation conditions are summarized in Table 2, where “ $\Delta$ ” represents a part of the structure could be confirmed. According to this result, three backscatter lines could not be observed for the illumination angle less than  $65^\circ$ , even its scale match the backscatter model shown in Fig. 1(a). The ambiguity was observed for Tsurumi-tsubasa bridge and Yokohama Bay bridge from the same Pi-SAR2 image. Thus, the acquisition condition is considered as a main reason for the ambiguity.

#### 4. BACKSCATTER CHARACTERISTICS OF SMALL BRIDGES

Twelve small bridges (No. 1-12) over Sumida river, Tokyo, Japan were used to observe the behaviours of small bridges in SAR images. Their locations are shown in Fig. 5, overlapping on one ascending and one descending TSX images. They includes most of the structure types, e.g. suspension, girder. The acquisition conditions of the two TSX images are shown in Table 1. Although the height information of some bridges lack, they all matched to the second backscatter model shown in Fig. 1(b). Thus, it is difficult to distinguish the three backscatter lines respectively. Here, we focused on the visibility of specular reflection from the deck and the clarity of the boundary. The specular reflection was judged by comparing the backscatter intensity of the bridge with that from the water. When the backscatter of the deck is lower than the mean value plus one standard deviation of the water, it is considered that the specular reflection occurred. The boundary was recognized by the strong backscatter of the handrails or parapets.

The behaviours of the twelve bridges are summarized in Table 3, sorted by the increase of the illumination angle. The specular reflection could be confirmed only when the illumination angle was small (less than  $15^\circ$ ). As mentioned in the previous section, the three backscatter lines occur more easily when the illumination angle is large. However, the three backscatter lines were overlapped for these small bridges. It was difficult to recognize the deck of the bridge from the overlapped backscatter intensity. Besides the influence of the illumination angle, the structure type of the bridge also affected the backscatter characteristics significantly. The multi-route composition and the superstructure of truss bridges make the backscatter model complex. The structure type will be considered in the future work.

Two samples are shown in Fig. 6. The first one is Ryogoku bridge (No. 2), which is a cantilever girder bridge. In the both TSX images, strong backscatter could be observed by the reflection of handrails. In the



(a) Descending (b) Ascending

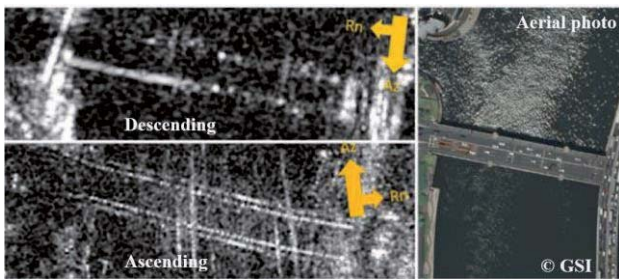
Figure 5. Twelve small bridges over Sumida river in the two TSX images

Table 3 Backscatter behaviours of the twelve small bridges

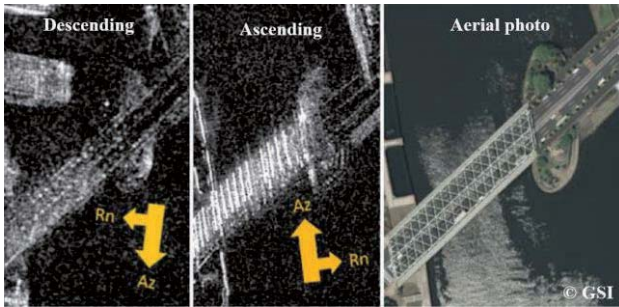
$\theta$ [ $^\circ$ ]	No.	Path	$\sigma^0$ (dB)	Specular reflection	Boundary
1	2	Des	-13.56	○	○
4	10	Asc	-12.67	○	○
5	7	Des	-12.45	○	○
15	1	Des	-8.88	×	○
16	10	Des	-12.67	○	○
17	6	Des	0.68	×	×
21	4	Asc	-6.40	×	○
21	2	Asc	-9.47	×	○
23	5	Des	-5.69	×	○
25	7	Asc	-9.09	×	○
33	9	Asc	-0.76	×	×
35	1	Asc	-7.71	×	○
37	6	Asc	-2.14	×	×
38	11	Des	-2.51	×	○
41	4	Des	-2.76	×	○
43	5	Asc	-5.41	×	○
44	12	Des	-1.67	×	○
53	9	Des	-4.78	×	○
58	11	Asc	-7.55	×	×
64	12	Asc	-6.53	×	○
50-68	8	Des	0.94	×	×
70-88	8	Asc	-3.39	×	○
48-90	3	Des	-1.46	×	×
33-90	3	Asc	-2.99	×	×

ascending TSX image with the illumination angle of  $21^\circ$ , the backscattering from the fences between the roadway and sidewalk also could be confirmed. However, the backscatter of multiple reflection is overlapped on the layover of the deck. The specular reflection could not be distinguished. In the descending image, the range direction was almost parallel to the bridge-axes. The overlapping of the multiple reflection does not occur. The specular reflection of the deck could be confirmed clearly by low backscattering between boundary lines.

The second one is Aioi bridge (No. 9), which is a truss girder bridge. In the descending TSX image with the



(a) Ryogoku bridge (No.2)



(b) Aioi bridge (No. 9)

Figure 6. Two samples of the small bridges.

illumination angle of  $53^\circ$ , the boundary of the bridge could be confirmed by the reflection of handrails. The overlap of the multiple reflection between the bridge and water caused high backscattering in the layover of the deck. Thus, the specular reflection could not be observed. In the ascending image with the illumination angle of  $33^\circ$ , the superstructure of the truss shows high backscatter and its layover overlapped on the backscatter of the deck. Both the specular reflection and the boundary could not be confirmed in this image.

## 5. CONCLUSIONS

In this study, the fundamental investigation on the backscatter models of bridges was carried out using sixteen bridges in three satellite and two aerial SAR images. Our aim is to develop a method for the bridge damage extraction from one post-event SAR scene after a disaster strikes.

By comparing the behaviours of four large bridges around Tokyo Bay, Japan, the large illumination angle makes the multiple reflection clear in the SAR images. The distance between the first, second and third backscatter line is determined by the incident angle. However, due to the specular reflection of a flat deck, it is difficult to judge the damage only by the low backscatter intensity.

The three backscatter lines could not be confirmed for the twelve target bridges due to their low heights from the water. When the illumination angle is larger than  $15^\circ$ , the backscatters from the multiple reflection are overlapped. It is difficult to detect the situation of the deck from the complex overlapped backscattering. The structure type of bridges exhibits important role, and thus, this issue will be considered in the future discussion.

## Acknowledgement

The TerraSAR-X images are the property of the German Aerospace Center (DLR) and Infoterra GmbH, and provided by PASCO Corporation, Tokyo, Japan. The Pi-SAR2 images are provided by the National Institute of Information and Communications Technology (NICT).

## References

Brett, P.T.B. and Guida, R., 2013. Earthquake damage detection in urban areas using curvilinear features. *IEEE Trans.Geosci. Remote Sens.*, 51, pp. 4877-4884.

Dong, L. and Shan, J., 2013. A comprehensive review of earthquake-induced building damage detection with remote sensing techniques. *ISPRS J. Photogramm. Remote Sens.*, 84, pp. 85-99.

Geospatial Information Authority of Japan (GSI): <https://maps.gsi.go.jp/#5/35.362222/138.731389/&base=std&ls=std&disp=1&vs=c1j0l0u0t0z0r0f0>

Lazecky, M. Hlavacova, I. Bakon, M. Sousa, J.J., Perissin, D. Patricio, G., 2017. Bridge Displacements Monitoring using Space-Borne SAR Interferometry. *IEEE Journal of Selected Topics in Applied Earth Observations and Remote Sensing*, 10(1), pp. 205-210.

Liu W. and Yamazaki F., 2011. Urban change monitoring by from multi-temporal TerraSAR-X images. *2011 Joint Urban Remote Sensing Event*, pp. 277-280.

Soergel, U., Gross, H., Thiele, A. and Thoennesen U., 2006. Extraction of bridges over water in multi-aspect high-resolution InSAR data. *International Archives of The Photogrammetry, Remote Sensing and Spatial Information Sciences*, XXXVI(3), pp. 185-190.

Sousa, J.J., Hlaváčová, I., Matúš, B., Lazecký, M., Patricio, G., Guimarães, P., Ruiz, A.M., Bastos, L., Sousa, A. and Bento, R., 2014. Potential of Multi-Temporal InSAR Techniques for Bridges and Dams Monitoring. *Journal of Procedia Technology*, 16, pp. 834-841.